analytical chemistry

pubs.acs.org/ac Article

Lipid Curvature and Fluidity Influence Lipid Incorporation Disparities in Nanodiscs

Marina C. Sarcinella, Joshua D. Jones, Matthew J. Sorensen, Samantha A. Edgcombe, Brandon T. Ruotolo, Robert T. Kennedy, and Ryan C. Bailey*

Cite This: *Anal. Chem.* 2025, 97, 2883−2889 Read Online

ACCESS | Metrics & More | Article Recommendations | Supporting Information

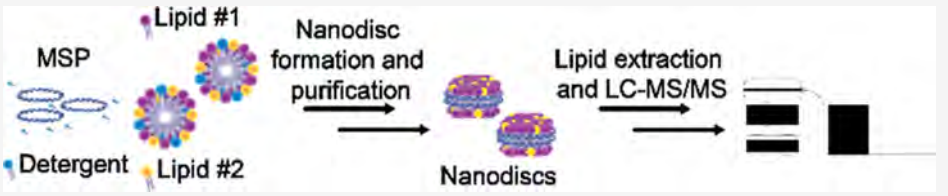

ABSTRACT: Nanodiscs have become a popular membrane mimetic system offering a well-defined bilayer environment to stabilize membrane proteins for in vitro analyses using a range of analytical methods; however, lipid compositions common to their deployment are simplistic and often fail to model native membrane complexity. Furthermore, there has been a general lack of rigorous analytical and biophysical characterization of nanodiscs comprising more than one lipid. To address these challenges, we coupled a nanodisc formation and purification workflow with targeted LC−MS/MS analysis to quantify lipids in nanodiscs made with different compositions. We screened lipids with a variety of headgroups and acyl chains and found that lipids did not always incorporate into nanodiscs at expected levels. Disparities in lipid incorporation were found to increase upon the addition of lipids known to induce curvature or rigidity to the membrane. Additionally, we found that adding just one additional type of lipid to nanodiscs changes the particle diameter and dispersity compared to nanodiscs containing a single lipid. We also formed and characterized nanodiscs using a complex starting composition inspired by the endoplasmic reticulum membrane and observed native-like cholesterol dynamics that modulated the lipid fluidity in the model bilayer system. Taken together, this work serves as a foundation for understanding nonstoichiometric lipid incorporation into nanodiscs and provides a basis for more thorough nanodisc characterization and quality control, which is critical to ensure multilipid nanodiscs synthesized accurately model the biological system of interest, enabling robust characterization of how the lipid landscape affects membrane protein structure and activity.

INTRODUCTION

Membrane proteins are important therapeutic targets since they are essential to a multitude of cellular processes such as signal transduction and metabolism.[1,2] Thus, in vitro membrane protein characterization is essential, but their propensity to misfold or aggregate in aqueous solutions makes them challenging to analyze. This has led to the development of membrane mimetic systems to stabilize membrane proteins in vitro and preserve their structure and activity.[3−8] One such mimic is the nanodisc, a discoidal lipid bilayer encircled by an amphipathic helical belt protein, membrane scaffold protein (MSP), that provides membrane proteins a stable, native-like bilayer that is structurally and compositionally defined.[9−11] Initially developed by Sligar and colleagues, this valuable model membrane construct self-assembles upon the removal of detergent from a solubilized component mixture containing a defined ratio of lipids, MSP, and membrane protein.[12−14]

Since their development, nanodiscs have found broad utility as membrane constructs to support the analytical characterization of all classes of membrane proteins using a multitude of techniques. Nanodiscs have enabled structural elucidation of membrane proteins utilizing tools such as X-ray crystallography, NMR, and cryo-electron microscopy.[9,10] Additionally, nanodiscs have facilitated membrane protein activity assays and studies that reveal membrane protein interactions with other proteins, lipids, and ligands using tools such as mass spectrometry, fluorescence assays, and surface sensitive techniques.[9,10,15] Consequently, the lipid composition of these nanodiscs will have an immense impact on the results of these characterization studies. We endeavored to robustly classify the lipid incorporation into nanodiscs to support their continued implementation in the membrane protein field.

To date, many studies utilizing nanodiscs have relied on simplistic bilayer compositions, primarily those solely contain-

Received: October 11, 2024
Revised: January 3, 2025
Accepted: January 7, 2025
Published: January 31, 2025

https://doi.org/10.1021/acs.analchem.4c05494
Anal. Chem. 2025, 97, 2883−2889

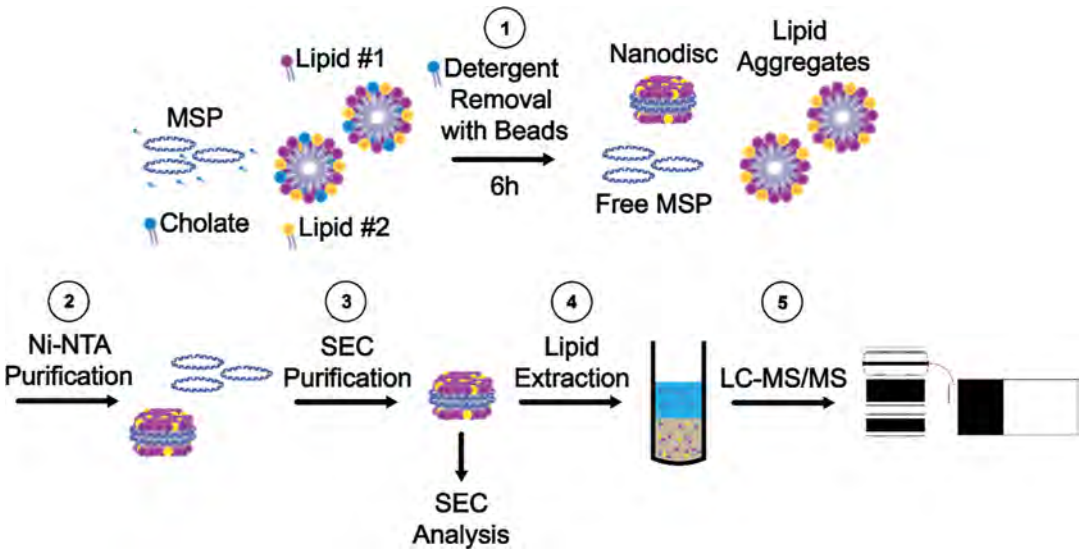

Figure 1. Nanodisc formation, purification, and analysis workflow. (1) Nanodiscs self-assemble upon detergent removal. (2) Nanodiscs are purified with Ni-NTA. (3) Nanodiscs are purified with SEC. From here, nanodisc samples are reinjected and analyzed via SEC. (4) For quantitative analysis, lipids are extracted from nanodiscs using a modified Bligh and Dyer protocol. (5) Lipids are separated with reverse phase liquid chromatography and quantified using multiple reaction monitoring on a triple quadrupole mass spectrometer.

ing phosphatidylcholine (PC) lipids. To better mimic the native membrane environment for membrane protein analyses, increased lipid complexity is needed.[16] More lipid-complex nanodiscs are especially important since specific lipids can allosterically modulate membrane protein activity.[17,18] There have been recent efforts toward this goal, but better characterization tools to quantify the lipid composition in nanodiscs are required to inform the rational synthesis of multilipid nanodiscs. Improved characterization methods are particularly essential, as certain phospholipid physical properties, such as the propensity to induce membrane fluidity and/or curvature, could hinder incorporation, resulting in nanodisc content that does not accurately reflect the input lipid stoichiometry. Additionally, knowledge of lipids that do not yield the intended compositions will help provide a better understanding of compositions that are predictable and amenable to nanodiscs. Recently, lipids presenting certain physiochemical characteristics were shown to incorporate into nanodiscs depending on synthesis conditions.[19] Previously, Marty and co-workers created nanodiscs modeling various native membranes with unique combinations of lipids that incorporate stoichiometrically and are amenable to native mass spectrometry,[20−22] theoretically enabling membrane protein characterization in a highly controlled environment. We sought to create a more straightforward characterization approach to analyze any abundant lipids found in phospholipid membranes commonly used in nanodisc synthesis that does not require access to the expensive instrumentation and specialized training necessary to perform native mass spectrometry.

To accomplish these goals, we combined a nanodisc formation and purification workflow with a targeted lipidomics method to quantify the lipids in nanodiscs of varying composition. We surveyed mixtures of lipids with different headgroups and acyl chains to determine the impacts of curvature and fluidity on the lipid composition in nanodiscs and their physical properties (e.g., diameter and dispersity). The incorporation of just one additional type of lipid significantly changed the diameter and dispersity of the resulting nanodiscs compared with 100% PC nanodiscs. We identified that lipids capable of inducing higher membrane curvature were present in lower, substoichiometric quantities compared to their expected levels. Additionally, PCs that impart greater membrane rigidity were also present in lower quantities than expected on the basis of the starting composition. We further expanded beyond binary lipid mixtures and created nanodiscs to model the endoplasmic reticulum membrane and observed the dynamics of cholesterol levels that reflect native membrane biology. These insights provide a foundation for a deeper understanding of lipid incorporation into nanodiscs by using established targeted LC−MS/MS techniques. Furthermore, this type of nanodisc characterization will likely be essential for further advances in this construct to enable the structural and/or functional characterization of membrane protein systems of increasing complexity.

MATERIALS AND METHODS

Materials. Amberlite XAD-2, cholesterol, HPLC grade chloroform, LC−MS grade 2-propanol, and LC−MS grade ammonium formate were purchased from Sigma-Aldrich. Sodium cholate, LC−MS grade acetonitrile, LC−MS grade formic acid, acetic acid, LC−MS grade methanol, potassium chloride, sodium chloride, sodium azide, Tris Base, and ethylenediaminetetraacetic acid were purchased from Fisher. 1-Palmitoyl-2-oleoyl-*glycero*-3-phosphocholine (POPC), 1,2-dimyristoyl-*sn*-glycero-3-phosphocholine (DMPC), 1,2-dipalmitoyl-*sn*-glycero-3-phosphocholine (DPPC), 1,2-distearoyl-*sn*-glycero-3-phosphocholine (DSPC), 1,2-dioleoyl-*sn*-glycero-3-phosphocholine (DOPC), 1-palmitoyl-2-oleoyl-*sn*-glycero-3-phospho-L-serine (POPS), 1-palmitoyl-2-oleoyl-*sn*-glycero-3-phosphate (POPA), 1-palmitoyl-2-oleoyl-*sn*-glycero-3-phosphoethanolamine (POPE), 1,2-dioleoyl-*sn*-glycero-3-phosphoethanolamine (DOPE), *N*-palmitoyl-D-*erythro*-sphingosylphosphorylcholine (SM), 1′,3′-bis[1,2-dioleoyl-*sn*-glycero-3-phospho]-glycerol (CL), 1,2-distearoyl-*sn*-glycero-3-phosphoinositol (PI) were purchased from Avanti Polar Lipids. MSP 1E3D1 (MSP) was purchased from Sigma-Aldrich (M7074) or expressed and purified as previously described.[14]

https://doi.org/10.1021/acs.analchem.4c05494
Anal. Chem. 2025, 97, 2883−2889

Nanodisc Assembly. Binary lipid nanodiscs were synthesized with 20, 40, 60, or 80% POPS, POPA, POPE, DOPE, SM, and CL (only 20 and 40%) balanced with POPC, or 20, 40, 60, or 80% DSPC, DPPC, DMPC, POPC, and DOPC balanced with POPS. Mitochondrial membrane nanodiscs were made with 50% POPC, 30% POPE, and 20% CL. Endoplasmic reticulum-inspired nanodiscs were made with 58% POPC, 20% POPE, 7% POPS, 7% PI, 4% SM, and 4% cholesterol.[23] In the case without cholesterol, 62% POPC was used. For the DPPC composition, it replaced POPC at 58% and all other lipids were kept the same.

Nanodiscs were assembled as previously described.[12,13] Briefly, chloroform-dissolved lipid mixtures in defined ratios were dried under nitrogen and stored in a desiccator overnight. The dried lipids were then solubilized at a concentration of 50 mM total lipid with 100 mM sodium cholate, except for DSPC nanodiscs where 200 mM cholate was used to solubilize lipids to 25 mM. Nanodiscs were assembled by adding MSP to the solubilized lipids diluted to 225 μL in standard disc buffer (20 mM Tris pH 7.4, 0.1 M NaCl, 0.5 mM EDTA, 0.01% NaN_3) and supplemented with sodium cholate to a final concentration of 20 mM. The final lipid concentration in the mixture was 5 mM and the lipid/MSP was 160:1 for POPC discs, 185:1 for DMPC discs, 210:1 for DPPC discs, and 235:1 for DSPC discs to ensure nanodiscs were fully lipidated.[24] The component mixture was incubated on an end-over-end mixer at room temperature for POPC (POPC nanodiscs with SM were made at 37 °C) and DMPC discs for 30 min. For DPPC and DSPC discs, an incubator was used at 41 and 55 °C, respectively. The mitochondrial membrane nanodiscs were made at room temperature, and the endoplasmic reticulum nanodiscs were made at 41 °C.

To the solubilized lipid/MSP mixture, 112 mg of Amberlite beads were added before incubating at their respective temperatures for 6 h before the solution was removed from the beads using a gel-loading pipet tip. Nanodiscs were then immediately purified with Ni-NTA spin columns (NEB). They were then further purified by size exclusion chromatography (SEC) using a Superdex Increase 200 3.2/300 column (Cytiva) on a Waters 2695 liquid chromatograph by injecting 50 μL of nanodiscs onto the column and pooling the fractions that contained the nanodisc peak (Figure 1). The mobile phase was a standard disc buffer.

Characterization of Nanodisc Size and Dispersity Using SEC. A 50 μL volume of the purified nanodisc sample was reinjected on the same column for size and dispersity analysis (Figures S1−S3). The Stokes diameters of the nanodiscs were determined using a calibration created from a protein standard solution (BioRad). For each nanodisc composition, the diameters were compared to that of a nanodisc containing 100% of the PC lipid. Percent change in dispersity was calculated by determining the difference in the diameters of the nanodiscs at full width at half-maximum (fwhm) on the front and back end of the nanodisc peak. This value was normalized to nanodiscs containing 100% of the PC lipid.

Sample Preparation and LC−MS/MS Analysis. Lipids were extracted from the dual-purified nanodiscs using a modification of the Bligh and Dyer extraction protocol (Figure 1).[25,26] To 25 μL of nanodisc sample in an Eppendorf tube, 100 μL of 0.15 M KCl in water, 200 μL of methanol, 100 μL of chloroform, and 0.5 μL of acetic acid (all cold) were added and vortexed. An additional 100 μL of water and 100 μL of chloroform (both cold) were then added and vortexed. The tubes were shaken at 4 °C for 10 min and then centrifuged at 12,100g for 5 min at 4 °C. A 150 μL volume of the organic layer was collected and transferred to an HPLC vial, dried under nitrogen gas, and reconstituted in 150 μL of mobile phase B. Samples were diluted within the range of mobile phase B.

The resulting lipids were separated using a Phenomenex Onyx Monolithic C18 column with a guard column at 400 μL/min on an Agilent 1290 Infinity II liquid chromatograph interfaced to an Agilent 6410 triple quadrupole mass spectrometer. Mobile phase A was 60/40 (v/v) water/acetonitrile with 10 mM ammonium formate and 0.1% (v/v) formic acid. Mobile phase B was 85/10/5 (v/v/v) 2-propanol/acetonitrile/water with 10 mM ammonium formate and 0.1% (v/v) formic acid. The gradient is displayed in Table S1. The autosampler was held at 15 °C, and 5 μL was injected for each sample. The eluting lipids were quantified using multiple reaction monitoring and ionized using electrospray ionization in positive mode at 4 kV or negative mode at −3.5 kV (Table S2). The gas temperature was 350 °C, the gas flow rate was 11 L/min, and the nebulizer gas pressure was 35 psi.

To quantify the lipids, calibration curves were created for each lipid species. DMPC (10 nM positive mode and 500 nM negative mode) was used as the internal standard for all analyses, unless DMPC was used for the nanodisc sample, in which case POPC (10 nM positive mode and 500 nM negative mode) was used as the internal standard. Automated peak integration was performed using Agilent MassHunter Workstation Quantitative Analysis Software. All of the peaks were visually inspected to ensure proper integration. The calibration curves were plotted as the $\log_{10}$[Response Ratio] versus the $\log_{10}$[Concentration (pM)] and the lipids were quantified using the resulting linear regression. Percent change was calculated using the eq 1, where impure nanodisc refers to lipids extracted from the crude nanodisc mixture before dual-purification (after Step 1 in Figure 1) and pure nanodisc refers to lipids extracted from the nanodiscs after dual-purification (after Step 3 in Figure 1). The standard error of the % change % PC was propagated from the individual replicates of the impure and pure nanodiscs.

$$\%\ \text{change}\ \%\ \text{PC} = \frac{\%\ \text{PC in impure nanodisc} - \%\ \text{PC in pure nanodisc}}{\%\ \text{PC in impure nanodisc}} \times 100\% \quad (1)$$

RESULTS AND DISCUSSION

Binary Lipid Nanodiscs are Larger and More Disperse. Previous reports have demonstrated that changes in nanodisc synthesis components can alter their physical properties.[12,13,24,27,28] To ascertain whether the addition of a second lipid to PC nanodiscs changes the physical properties of nanodiscs, we made nanodiscs containing POPC with increasing amounts of POPS, POPA, POPE, DOPE, SM, and CL to survey the effects of different headgroups. Purified nanodiscs were analyzed via SEC, which was calibrated with protein standards to determine the nanodisc diameter. Change in dispersity was measured by determining the diameter range of the nanodiscs at fwhm and comparing that to nanodiscs made with 100% PC. In almost all cases (POPE, POPA, POPE, DOPE, and CL), the addition of a second lipid in any

https://doi.org/10.1021/acs.analchem.4c05494
Anal. Chem. 2025, 97, 2883−2889

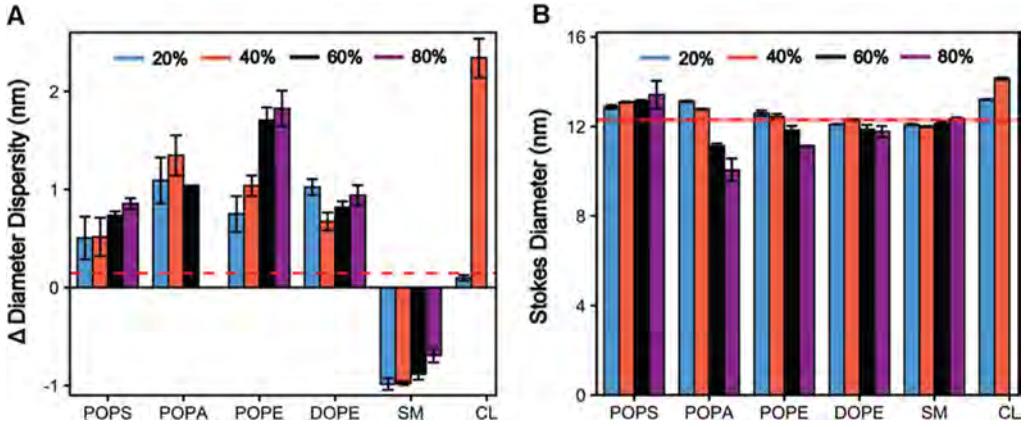

Figure 2. Diameter and dispersity of binary lipid nanodiscs with phospholipids with varying headgroups and a sphingolipid balanced with POPC. (A) Change in diameter dispersity of nanodiscs made with different lipid compositions. (B) Stokes diameter of nanodiscs made with different lipid compositions. The red dash indicates the average diameter of 100% POPC nanodiscs and the shaded region is the standard deviation of three replicate nanodisc preparations. Error bars are shown as the standard deviation of three replicate nanodisc assemblies.

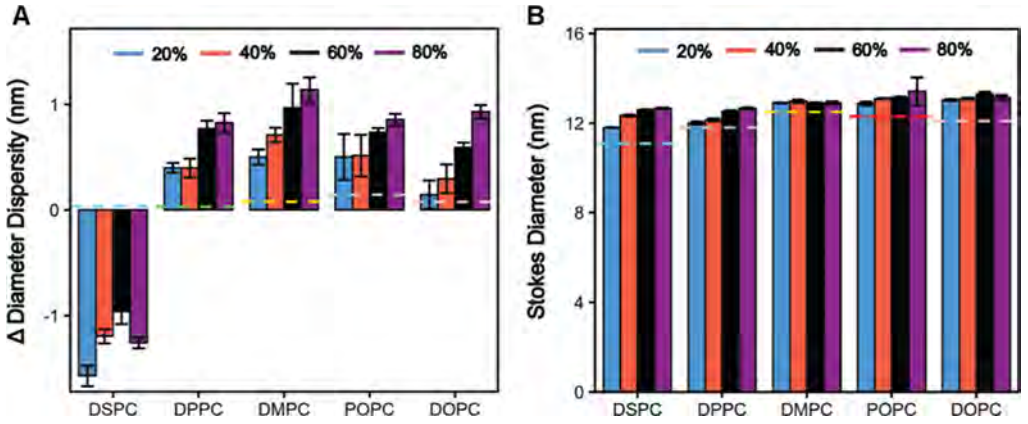

Figure 3. Diameter and dispersity of binary lipid nanodiscs with POPS balanced with PCs that impart varying membrane fluidity. (A) Change in diameter dispersity of nanodiscs made with different lipid compositions. (B) Stokes diameter of nanodiscs made with different lipid compositions. The dashed line indicates the average diameter of nanodiscs made with 100% of the respective PC lipid and the shaded region represents the standard deviation of three replicate nanodisc assemblies. Error bars are shown as the standard deviation of three replicate nanodisc assemblies.

amount significantly increased the dispersity of nanodiscs relative to the 100% POPC nanodiscs, with higher percentages for most lipids ranging between 1 and 2.5 nm more disperse (Figure 2A). This increase in dispersity is likely due to differences in lipid shape, leading to altered lipid incorporation and packing, allowing for a wider variety of particles with different numbers of lipids. This finding is supported by previous work showing that large quantities of anionic and PE lipids can alter the nanodisc populations produced.[20,21] Contrarily, SM containing nanodiscs were less disperse than the 100% POPC (Figure 2A), perhaps due to SM's propensity to strongly hydrogen bond and associate with raft domains.[29,30]

Additionally, adding in a second lipid to create a binary nanodisc changes the resulting diameter of the particles (Figure 2B), either increasing or decreasing it, depending on the identity and amount of the lipid added. In many cases, the 20 and 40% compositions had little change in diameter, but for some lipids, 60 and 80% significantly increased (like POPS, CL) or decreased (POPE, DOPE, POPA) the size of the nanodiscs relative to nanodiscs made with 100% POPC. In most cases (e.g., PA and PE), the nanodiscs trended smaller as the dispersity increased. This observation is likely due to these lipids not incorporating fully into nanodiscs resulting in a wider range of lipidation, with many nanodiscs underlipidated when highly curved lipids are incorporated.

In addition to determining the effect of lipid headgroups, phospholipid fluidity could further alter the synthesis of binary nanodiscs. To identify this effect, nanodiscs were made containing POPS with varying amounts of DMPC, DPPC, DSPC, POPC, and DOPC to determine the effects of different acyl chains. In nearly all cases, adding POPS to nanodiscs made with PCs with varying acyl chains led to similarly increased nanodisc dispersity (Figure 3A). Only with DSPC were the nanodiscs less disperse relative to 100% DSPC, likely due to the challenges in making 100% DSPC nanodiscs due to its high transition temperature. All nanodiscs made with varying acyl chains showed increased diameters relative to the 100% PC. Additionally, it is evident that the different PCs used to make the nanodiscs result in different diameter particles, with PCs that impart more membrane rigidity having smaller diameters (Figure 3B), likely due to the tighter packing capabilities of these lipids. Taken altogether, small changes in the lipid composition can lead to altered physical properties of nanodiscs, which in turn could affect both membrane protein incorporation and the structure and/or function of membrane proteins after incorporation.

https://doi.org/10.1021/acs.analchem.4c05494
Anal. Chem. 2025, 97, 2883−2889

Nanodiscs Containing Curved Lipids Show Disparities in Lipid Incorporation. While multilipid nanodiscs have been produced for membrane protein analyses by combining different lipids in the preassembly component mixture, the actual lipid composition of the resulting nanodiscs is typically not characterized. Since lipid headgroup and fluidity can affect nanodisc physical characteristics, we sought to identify whether the resulting nanodiscs contained the expected lipid composition reflective of the initial component mixture. To investigate the addition of other lipids to PC-based nanodiscs, we surveyed lipids with varying headgroups: PS, PA, PE, CL, and a sphingolipid, SM. We first established a nanodisc synthesis and dual purification workflow to ensure there were no excess lipids present to convolute our analyses (Figures 1, S1−S3). While many nanodisc analyses utilize only SEC purification, we incorporated Ni-NTA purification to enrich His_6-tagged nanodiscs and remove excess lipids. We then developed a targeted LC−MS/MS method to quantify lipids in purified nanodiscs to determine any disparities in lipid incorporation when these other lipids were added to the component mixture (Figures S4−S6).

We compared the percentage of POPC in the impure and pure nanodisc samples for multiple compositions for each binary mixture of lipids. Comparing to the percentage in the impure mixture allowed us to account for slight deviations in the starting composition away from the 20, 40, 60, and 80% and any lipid loss during solubilization or incubation, as only the lipids in the impure nanodisc mixture had the opportunity to incorporate into the nanodiscs. We found that in nearly all cases, there is enrichment of POPC relative to the intended amount of POPC added to the component mixture (Figure 4A). This enrichment was generally greater as the percentage of the second lipid was increased in the component mixture and could be as high as 15−30%, as was the case for POPA, POPE, DOPE, and CL. Nanodiscs made with PE lipids showed the greatest POPC enrichment between 25 and 30%. Some lipids such as POPS and SM showed little to no change from the input composition. These results are correlated with lipid shape, as conical lipids (POPA, DOPE, POPE, CL) that impart more curvature on the membrane were depleted in the purified nanodiscs when present in greater percentages of the total lipid composition. These results trend with lipid intrinsic curvature values determined in supported lipid bilayers.[31,32] For each lipid headgroup, the POPC enrichment for the 20% POPC condition was compared to the spontaneous curvature of each lipid. Lipid headgroups with greater curvature, particularly negative curvature such as PE and PA, had the greatest disparity in lipid incorporation (Figure S7). As these lipids are usually added to nanodiscs to ascertain their effect on membrane protein structure and function, it is critical to confirm these compositions to enable correlation of these changes with specific lipid compositions. While all lipids tested can be incorporated, we found their resulting compositions do not fully represent the input. Thus, analytical characterization of multilipid nanodisc composition will be extremely important to identify effects of lipids associated with membrane proteins.

Nanodiscs Containing Lipids with Varying Acyl Chains Show Disparities in Lipid Incorporation. In previous work with multilipid nanodiscs, it has been more common to add lipids with different headgroups but not different chain types. In addition to associating with various lipid headgroups, membrane proteins also interact with areas of the membrane that are more rigid or fluid.[16] To draw

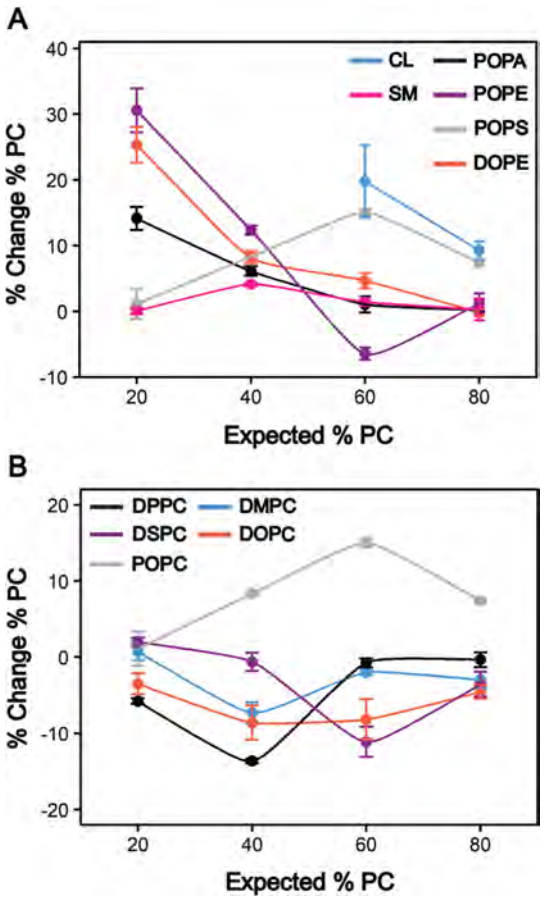

Figure 4. Quantitation of lipids in nanodiscs made with binary lipid mixtures. (A) Percent change of POPC measured in nanodiscs made with POPC and lipids of varying headgroups. (B) Percent change of PC measured in nanodiscs made with POPS and PCs of varying fluidity. Error bars are shown as the standard error of three replicate nanodisc assemblies. Δ % PC values can be found in Tables S3 and S4.

correlations between these interactions and changes in the membrane protein structure or function, it is important to evaluate these compositions as well. We surveyed nanodisc synthesis containing PCs with different chain lengths and unsaturations and made nanodiscs with POPS, a generally robust and popular secondary lipid for nanodiscs. We found that lipids that produce more rigid membranes showed an opposite trend to POPC, where the POPS was generally enriched (Figure 4B). Comparing DMPC to DPPC and DSPC, it is evident that PS is enriched with increasing PC rigidity. For DSPC, the PS enrichment was greater at higher percentages of DSPC, likely because the high transition temperature of the lipid makes the formation of higher percentage DSPC nanodiscs less favorable. For DOPC, which has two degrees of unsaturation, POPS was also enriched, likely showing that lipids with multiple kinks do not incorporate as favorably into nanodiscs as lipids with a single degree of unsaturation like POPC. These results show that despite the lipids having the same headgroup, they incorporate differently based on their acyl chains, as lipids that create more rigid membranes were depleted in the purified nanodisc samples, perhaps to modulate the fluidity of the bilayer.

Increased Lipid Complexity in Nanodiscs Models Native Organelle Membrane Interactions. Most pub-

https://doi.org/10.1021/acs.analchem.4c05494
Anal. Chem. 2025, 97, 2883−2889

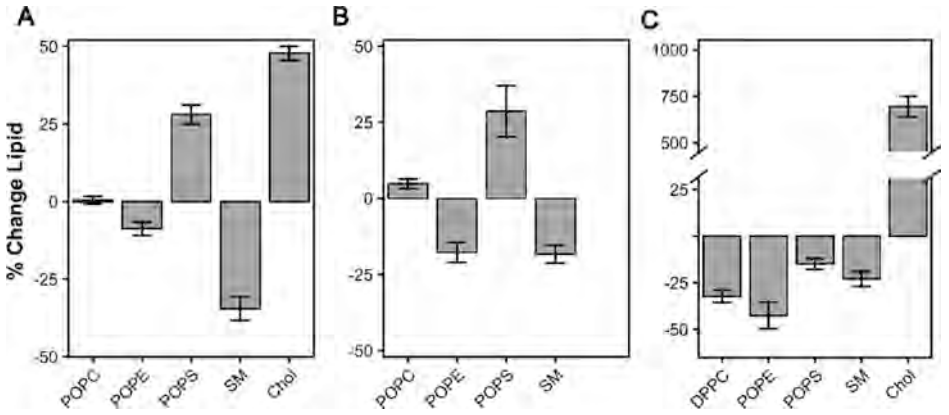

Figure 5. Quantitation of lipids in ER lipid mixture nanodiscs. (A) Nanodiscs made with ER mixture containing POPC. (B) Nanodiscs made with same mixture as in (A), but without cholesterol. (C) Nanodiscs made with same mixture as in (A), but with DPPC instead of POPC. Error bars are shown as the standard error of three replicate nanodisc assemblies.

lished studies using multilipid nanodiscs have focused on binary mixtures, though some studies have included compositions with three or more lipids. It is important to increase the complexity of the lipid composition in nanodiscs to study membrane proteins in more native-like environments. To increase the complexity of the lipid composition beyond binary mixtures, we synthesized nanodiscs to model the inner mitochondrial membrane and the endoplasmic reticulum membrane. The mitochondrial membrane nanodiscs contained a mixture of 50% POPC, 30% POPE, and 20% CL to model the native mitochondrial membrane composition,[33] but it is evident that there was significant depletion of CL compared to the intended composition, likely due to the large size and shape of CL (Figure S8). The endoplasmic reticulum nanodiscs contained a mixture of 58% POPC, 20% POPE, 7% POPS, 7% PI, 4% SM, and 4% cholesterol to model the native endoplasmic reticulum membrane as previously described.[23] We observe marked enrichment of cholesterol and depletion of SM compared to the input compositions, perhaps to equilibrate to an intermediate liquid ordered phase (Figure 5A).[34] When we made the same nanodisc mixture without cholesterol, we saw less depletion of SM (Figure 5B). Similar trends were seen in styrene maleic acid copolymer nanodiscs made with an equimolar ternary mixture of PC, SM, and cholesterol.[35]

We also investigated how incorporating a more rigid PC lipid into the ER mixture would affect lipid incorporation; therefore, we chose to introduce the more rigid DPPC. Under these conditions, we saw astonishingly high enrichment of cholesterol in these nanodiscs (Figure 5C). Due to the increased rigidity of DPPC relative to POPC, this DPPC nanodisc lipid mixture is more raft-like. Rafts are cholesterol-rich domains in native membranes,[30] and cholesterol has been shown to associate more with highly saturated PCs in other model membrane systems.[36] We also found generally that there was greater variability across replicates when we made nanodiscs with more than two lipid components. This means that our method would be less able to distinguish smaller changes in lipid composition with increasing complexity. More importantly, the variability in the lipid content could have greater ramifications for membrane protein study replicates as they could show reduced precision depending on lipid environment changes in the nanodisc. These ramifications are essential for the field to consider, as membrane proteins are studied in more complex lipid compositions.

CONCLUSIONS

With the increased need and interest in in vitro membrane protein characterization, increased lipid complexity that better models the native membrane in mimics such as nanodiscs is vital. Since nanodiscs have mainly been synthesized using single PC lipids, not much is known about the changes in physical properties or lipid composition upon the addition of other lipids to the component mixture. This work provides foundational analytical and biophysical characterization of multilipid nanodiscs. We surveyed lipids with different headgroups and acyl chains in binary mixtures with PC and identified that the resulting nanodiscs were often larger and more dispersed via SEC analysis. Further, we developed and applied a targeted LC−MS/MS assay that enables facile determination of lipid ratios in the nanodiscs, allowing a comparison against the composition of the starting lipid mixture. We found that the nanodisc composition often deviated from the input mixture, especially when lipids were contained with greater intrinsic curvature and with increased membrane rigidity. We further found that when increasing nanodisc complexity to model the ER membrane mixture, the lipid incorporation into nanodiscs was more variable, but we detected native-like cholesterol dynamics when modeling a less fluid membrane. Both changes in physical properties and disparities in lipid composition could influence membrane protein incorporation and activity, so it is critical that we understand and expect these changes and work to assess their impact on membrane proteins. We also hope this work serves as a foundation to better understand how multilipid nanodiscs are formed and for better characterization and quality control in nanodisc studies.

ASSOCIATED CONTENT

Supporting Information

The Supporting Information is available free of charge at https://pubs.acs.org/doi/10.1021/acs.analchem.4c05494.

Additional experimental details (PDF)

https://doi.org/10.1021/acs.analchem.4c05494
Anal. Chem. 2025, 97, 2883−2889

AUTHOR INFORMATION

Corresponding Author

Ryan C. Bailey − *Department of Chemistry, University of Michigan, Ann Arbor, Michigan 48109, United States;* orcid.org/0000-0003-1021-4267; Email: ryancb@umich.edu

Authors

Marina C. Sarcinella − *Department of Chemistry, University of Michigan, Ann Arbor, Michigan 48109, United States*

Joshua D. Jones − *Department of Chemistry, University of Michigan, Ann Arbor, Michigan 48109, United States;* orcid.org/0000-0002-8811-1340

Matthew J. Sorensen − *Department of Chemistry, University of Michigan, Ann Arbor, Michigan 48109, United States*

Samantha A. Edgcombe − *Department of Chemistry, University of Michigan, Ann Arbor, Michigan 48109, United States*

Brandon T. Ruotolo − *Department of Chemistry, University of Michigan, Ann Arbor, Michigan 48109, United States;* orcid.org/0000-0002-6084-2328

Robert T. Kennedy − *Department of Chemistry, University of Michigan, Ann Arbor, Michigan 48109, United States;* orcid.org/0000-0003-2447-7471

Complete contact information is available at: https://pubs.acs.org/10.1021/acs.analchem.4c05494

Author Contributions

Marina C. Sarcinella: conceptualization, methodology, investigation, formal analysis, writing—original draft, writing—review and editing, and visualization. Joshua D. Jones: methodology, investigation, formal analysis, writing—review and editing, and visualization. Matthew J. Sorensen: methodology, and writing—review and editing. Samantha A. Edgcombe: investigation and writing—review and editing. Brandon T. Ruotolo: writing—review and editing. Robert T. Kennedy: writing—review and editing. Ryan C. Bailey: conceptualization and writing—review and editing.

Notes

The authors declare no competing financial interest.

ACKNOWLEDGMENTS

We thank the following funding sources for their support: National Institute of General Medical Sciences of the National Institute of Health (GM138620 to R.C.B. and B.T.R.) and the National Science Foundation (GFRP to J.D.J. and NSF CHE 1904146 to R.T.K.). We thank Laura Snyder and Kristin Koutmou for their help expressing and purifying membrane scaffold protein.

REFERENCES

(1) Yıldırım, M. A.; Goh, K.-I.; Cusick, M. E.; Barabási, A.-L.; Vidal, M. *Nat. Biotechnol.* **2007**, *25* (10), 1119−1126.

(2) Overington, J. P.; Al-Lazikani, B.; Hopkins, A. L. *Nat. Rev. Drug Discovery* **2006**, *5* (12), 993−996.

(3) Seddon, A. M.; Curnow, P.; Booth, P. J. *Biochim. Biophys. Acta, Biomembr.* **2004**, *1666* (1−2), 105−117.

(4) Garavito, R. M.; Ferguson-Miller, S. *J. Biol. Chem.* **2001**, *276* (35), 32403−32406.

(5) Popot, J.-L. *Annu. Rev. Biochem.* **2010**, *79* (1), 737−775.

(6) Akbarzadeh, A.; Rezaei-Sadabady, R.; Davaran, S.; Joo, S. W.; Zarghami, N.; Hanifehpour, Y.; Samiei, M.; Kouhi, M.; Nejati-Koshki, K. *Nanoscale Res. Lett.* **2013**, *8* (1), 102.

(7) Sebaaly, C.; Greige-Gerges, H.; Charcosset, C. Lipid Membrane Models for Biomembrane Properties' Investigation. In *Current Trends and Future Developments on (Bio-) Membranes*; Basile, A., Charcosset, C., Eds.; Elsevier, 2019; Chapter 11, pp 311−340.

(8) Shen, H.-H.; Lithgow, T.; Martin, L. *Int. J. Mol. Sci.* **2013**, *14* (1), 1589−1607.

(9) Denisov, I. G.; Sligar, S. G. *Chem. Rev.* **2017**, *117* (6), 4669−4713.

(10) Denisov, I. G.; Sligar, S. G. *Nat. Struct. Mol. Biol.* **2016**, *23* (6), 481−486.

(11) Bayburt, T. H.; Sligar, S. G. *FEBS Lett.* **2010**, *584* (9), 1721−1727.

(12) Bayburt, T. H.; Grinkova, Y. V.; Sligar, S. G. *Nano Lett.* **2002**, *2* (8), 853−856.

(13) Denisov, I. G.; Grinkova, Y. V.; Lazarides, A. A.; Sligar, S. G. *J. Am. Chem. Soc.* **2004**, *126* (11), 3477−3487.

(14) Ritchie, T. K.; Grinkova, Y. V.; Bayburt, T. H.; Denisov, I. G.; Zolnerciks, J. K.; Atkins, W. M.; Sligar, S. G. *Methods Enzymol.* **2009**, *464*, 211−231.

(15) Marty, M. T. *Int. J. Mass Spectrom.* **2020**, *458*, 116436.

(16) Harayama, T.; Riezman, H. *Nat. Rev. Mol. Cell Biol.* **2018**, *19* (5), 281−296.

(17) Cong, X.; Liu, Y.; Liu, W.; Liang, X.; Laganowsky, A. *Nat. Commun.* **2017**, *8* (1), 2203.

(18) Dawaliby, R.; Trubbia, C.; Delporte, C.; Masureel, M.; Van Antwerpen, P.; Kobilka, B. K.; Govaerts, C. *Nat. Chem. Biol.* **2016**, *12* (1), 35−39.

(19) Odenkirk, M. T.; Zhang, G.; Marty, M. T. *J. Am. Soc. Mass Spectrom.* **2023**, *34* (9), 2006−2015.

(20) Kostelic, M. M.; Zak, C. K.; Jayasekera, H. S.; Marty, M. T. *Anal. Chem.* **2021**, *93* (14), 5972−5979.

(21) Hoi, K. K.; Robinson, C. V.; Marty, M. T. *Anal. Chem.* **2016**, *88* (12), 6199−6204.

(22) Kostelic, M. M.; Ryan, A. M.; Reid, D. J.; Noun, J. M.; Marty, M. T. *J. Am. Soc. Mass Spectrom.* **2019**, *30* (8), 1416−1425.

(23) Barnaba, C.; Ravula, T.; Medina-Meza, I. G.; Im, S.-C.; Anantharamaiah, G. M.; Waskell, L.; Ramamoorthy, A. *Chem. Commun.* **2018**, *54* (49), 6336−6339.

(24) Skar-Gislinge, N.; Johansen, N. T.; Høiberg-Nielsen, R.; Arleth, L. *Langmuir* **2018**, *34* (42), 12569−12582.

(25) Bligh, E. G.; Dyer, W. J. *Can. J. Biochem. Physiol.* **1959**, *37* (8), 911−917.

(26) Retra, K.; Bleijerveld, O. B.; van Gestel, R. A.; Tielens, A. G. M.; van Hellemond, J. J.; Brouwers, J. F. *Rapid Commun. Mass Spectrom.* **2008**, *22* (12), 1853−1862.

(27) Skar-Gislinge, N.; Simonsen, J. B.; Mortensen, K.; Feidenhans'l, R.; Sligar, S. G.; Lindberg Møller, B.; Bjørnholm, T.; Arleth, L. *J. Am. Chem. Soc.* **2010**, *132* (39), 13713−13722.

(28) Schachter, I.; Allolio, C.; Khelashvili, G.; Harries, D. *J. Phys. Chem. B* **2020**, *124* (33), 7166−7175.

(29) Barenholz, Y.; Thompson, T. E. *Chem. Phys. Lipids* **1999**, *102* (1), 29−34.

(30) Simons, K.; Ikonen, E. *Nature* **1997**, *387* (6633), 569−572.

(31) Kollmitzer, B.; Heftberger, P.; Rappolt, M.; Pabst, G. *Soft Matter* **2013**, *9* (45), 10877.

(32) Zimmerberg, J.; Kozlov, M. M. *Nat. Rev. Mol. Cell Biol.* **2006**, *7* (1), 9−19.

(33) Horvath, S. E.; Daum, G. *Prog. Lipid Res.* **2013**, *52* (4), 590−614.

(34) Ma, Y.; Ghosh, S. K.; DiLena, D. A.; Bera, S.; Lurio, L. B.; Parikh, A. N.; Sinha, S. K. *Biophys. J.* **2016**, *110* (6), 1355−1366.

(35) Dominguez Pardo, J. J.; Dörr, J. M.; Iyer, A.; Cox, R. C.; Scheidelaar, S.; Koorengevel, M. C.; Subramaniam, V.; Killian, J. A. *Eur. Biophys. J.* **2017**, *46* (1), 91−101.

(36) Silvius, J. R. *Biochim. Biophys. Acta, Biomembr.* **2003**, *1610* (2), 174−183.